

DETC2005/VIB-84520

FREQUENCY RESPONSE OF VIBRATION ISOLATORS WITH SATURATING SPRING ELEMENTS

Mahinfalah, M., M.Mahinfalah@ndsu.edu

G. Nakhaie Jazar, Reza.N.Jazar@ndsu.edu

M. Rastgaar Aagaah, Aagaah.Rastgaar@ndsu.edu

N. Mahmoudian, Nina.Mahmoudian@ndsu.edu

Dept. of Mech. Eng. North Dakota State University, Fargo, ND, 58105

KEYWORDS: vibration isolators, piecewise linear system, nonlinear system, saturation characteristics.

Abstract

An investigation using averaging method is carried out to obtain the frequency response of a class of vibration isolators with saturation spring. The saturation characteristics are modeled using a hyperbolic-tangent function. The hyperbolic-tangent saturation function is compared with other popular saturation functions, using piecewise nonlinear approximation. A parameteric study indicates that piecewise linear approximation of saturating functions provide results that are close enough to the results of hyperbolic tangent approximation. A sensitivity analysis of frequency response of the system is also investigated based on the piecewise linear approximation.

1. INTRODUCTION

Figure 1 depicts mechanical model of a one degree-of-freedom suspension system. Recently a new type of damper with a saturation characteristic has been introduced in vibration optimization community. Using Magneto Rheological (MR) fluids and applying an electric current, the damping coefficient of the damper can be controlled almost linearly within a specific range of velocity. However, the force of the damper will be saturated when the velocity approaches a critical value called "breaking velocity" (Jolly 1996), and additional force will be developed when the velocity exceeds the breaking velocity (Jolly et. al. 1996).

Magneto Rheological (MR) and Electro Rheological (ER) fluids also show a saturating stiffness behavior i.e., a

saturating spring. Saturating stiffness phenomenon are generally a characteristic occurring in magnetic field and result in enhancement of shear stress developed within the fluid, as well as dry friction dampers. This property is also employed to control the cantilever magnetometry, (Chabota, and Moreland 2003), hydraulic springs (Walsh, and Lamancusa 1992) and electro-mechanical valves actuators (Tai, Stubbs, and Tsao 2001). Also, inclusion of the stick-slip and hysteresis in the model of dry friction law during the slip phase, creates a creep force that saturates at the adhesion limit value. This is a model utilized in the dynamics resulting from the coupling between the nonlinearities in the dry friction model, and the impact with the guidance of railways (True, and Asmund 2002).

In this paper a vibration isolation system employing a nonlinear cubic spring along with a saturation spring in parallel with a linear viscous damper is studied under base excitation. The behavior of such a system can be described by the following equation of motion.

$$u'' + a_1 u' + u + a_2 u^3 + a_3 \tanh(a_4 u) = r^2 \sin(r \tau)$$

The steady state frequency-amplitude dependency of the system is derived by applying the averaging method. The analytical results have been utilized to investigate the parameter sensitivity. The main outcome of this analysis would be comparison of the smooth saturating model with piecewise linear saturating model. Also it will be demonstrated that the piecewise linear model reserves the main dynamic characteristics of the saturating spring phenomenon.

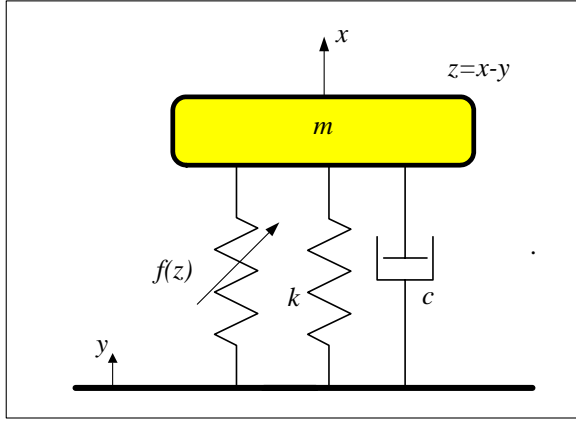


Figure 1. Mechanical model of a suspension system using traditional and saturated spring and damper.

Different analytic functions are available to describe a saturating phenomenon. The most popular functions are illustrated in Figure 2, and are compared to piecewise linear saturating model. The analytic descriptions of the saturating functions are as follow.

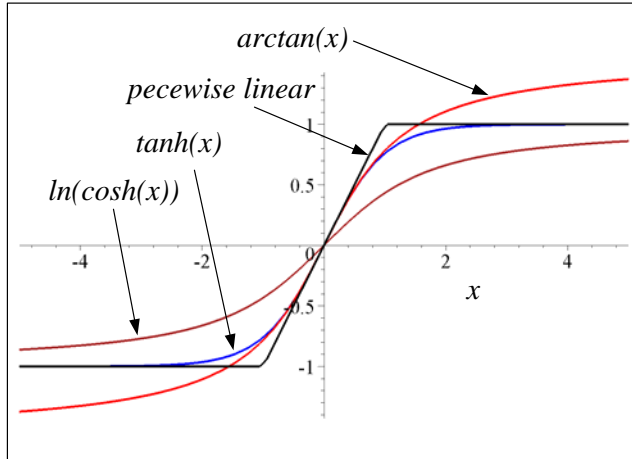


Figure 2: Illustration of saturated functions

a. *Hyperbolic-tangent type*

$$F_1(x) = a \tanh(bx) \quad (1)$$

b. *Arc-tangent type*

$$F_2(x) = a \tan^{-1}(bx) \quad (2)$$

c. *Hyperbolic -cosine type*

$$F_3(x) = a \ln(\cosh(bx)) \quad (3)$$

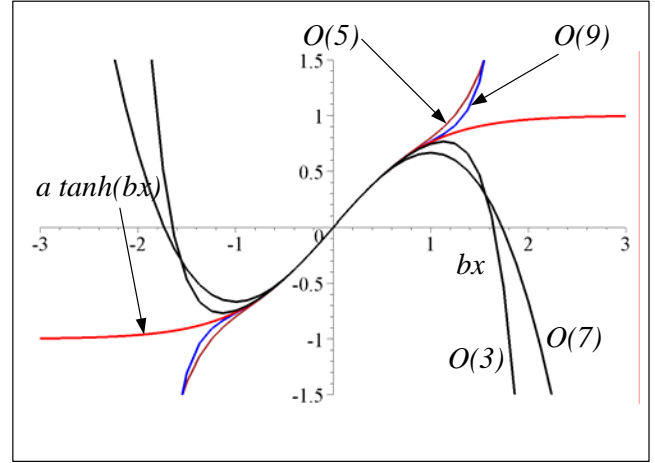


Figure 3: Comparison of different approximation orders for a hyperbolic-tangent function

The maximum force of the saturating spring and the breaking amplitudes are functions of the control characteristics, which are embedded in parameters a and b . Experimental investigations show that hyperbolic-tangent describes the behavior of a saturating spring and damper more accurately.

Figure 3 compares the hyperbolic-tangent with its series approximation of different order. It is shown that increasing the order of expansion does not represent the saturation behavior of the function. Hence, instead of a continuous function approach, we employ a piecewise nonlinear function approach.

Using a Taylor series the hyperbolic-tangent function was expanded into a polynomial function.

$$a \tanh(bx) = abx - \frac{1}{3}ab^3x^3 + \frac{2}{15}ab^5x^5 - \frac{17}{315}ab^7x^7 + \frac{62}{2835}ab^9x^9 + O(x^{11}) \quad (4)$$

Three different expansion will be utilized to describe the saturating function within the limits of working amplitudes. The first function is found by expanding the hyperbolic-tangent function about $x=0$.

$$f_1 = a \tanh(bx) \Big|_{x=0} = abx - \frac{1}{3}ab^3x^3 \quad (5)$$

Two other functions f_2 , and f_3 may be developed by expansion at two arbitrary positions δ_0 and $-\delta_0$ and accepting another third order polynomials. The switching amplitude δ_0 may be selected to provide the best curve fitting. Expanded functions f_1 , f_2 , and f_3 are illustrated in

Figure 4. Accepting f_1 for $-\delta_0 \leq bx \leq \delta_0$, f_2 for $\delta_0 \leq bx < \delta_1$, and f_3 for $-\delta_1 < bx \leq -\delta_0$, where $\delta_1=2$ and $\delta_0 < 1$ is a user defined fixed value, provide a piecewise nonlinear approximation of the saturating function.

$$a \tanh(bx) = a f(bx) = \begin{cases} a & 2 < bx \\ f_2 & \delta_0 \leq bx \leq 2 \\ f_1 & -\delta_0 \leq bx \leq \delta_0 \\ f_3 & -2 \leq bx \leq -\delta_0 \\ -a & bx < -2 \end{cases} \quad (6)$$

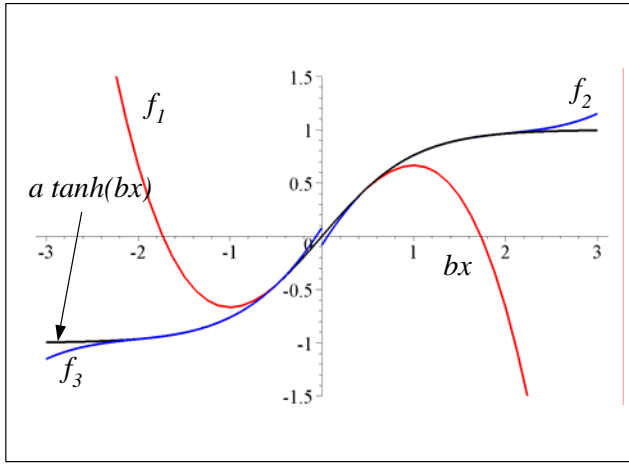


Figure 4: Expanded functions f_1 , f_2 , and f_3 .

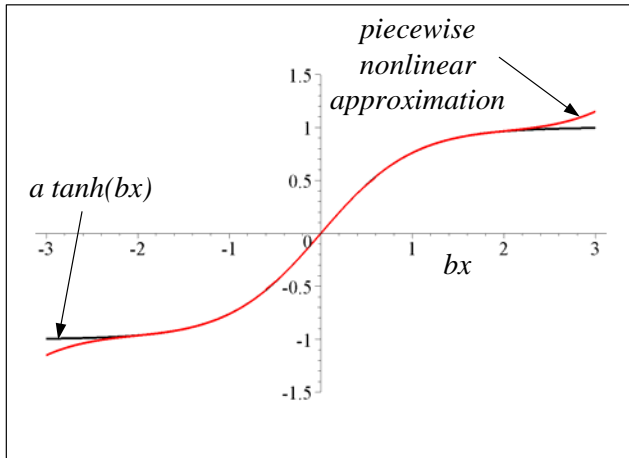


Figure 5: Comparison of hyperbolic-tangent function and its piecewise nonlinear approximation.

The functions f_2 , and f_3 and their derivatives have to satisfy the continuity conditions with respect to f_1 and

saturated values at joining points $x = \pm\delta_0/b$ and $x = \pm 2/b$.

The approximated piecewise nonlinear function (6) is illustrated in Figure 5 and is compared with the hyperbolic-tangent function. The limit values of δ_0 for switching functions f_2 , and f_3 is selected based on $|a \tanh(bx) - f_2| < 0.001$, although it could also be found by minimization of the error function $e = |a \tanh(bx) - f_2|$. Whenever the absolute value of the argument bx passes the limit values then $\tanh(bx)$ is assumed to be one.

Assuming a nonlinear third order function for the primary spring, and a linear characteristic for the primary damper, the equation of motion of the system shown in Figure 1 would be:

$$m\ddot{x} + c(\dot{x} - \dot{y}) + k_1(x - y) + k_2(x - y)^3 + a \tanh(b(x - y)) = 0 \quad (7)$$

Introducing a relative displacement coordinate $z=x-y$, and employing a set of dimensionless parameters, the equation of motion transforms to the following equation,

$$u'' + a_1 u' + u + a_2 u^3 + a_3 \tanh(a_4 u) = r^2 \sin(r\tau) \quad (8)$$

where

$$a_3 = \frac{a}{k_1 Y} \quad \frac{z}{Y} = u \quad \omega_1 = \sqrt{\frac{k_1}{m}} \quad \omega_1 t = \tau \quad r = \frac{\omega}{\omega_1} \quad a_4 = bY$$

$$y = Y \sin(\omega t) \quad a_1 = \frac{c}{\sqrt{k_1 m}} \quad a_2 = \frac{k_2 Y^2}{k_1} \quad x - y = z \quad (9)$$

2. FREQUENCY RESPONSE

2.1. Nonlinear Spring, No Saturation

Setting $a_3=0$ in Equation (8), the problem reduces to a base excited Duffing-type vibration isolator.

$$u'' + a_1 u' + u + a_2 u^3 = r^2 \sin(r\tau) \quad (10)$$

A closed form equation describing the frequency response of the system (10) may be found using a perturbation and

approximation method such as averaging method (Nayfeh and Mook 1979, Tondle 1986).

$$9a_2^2U^6 + 24(a_1 - a_2^2r^2)U^4 + 16(1 + r^4 - 2r^2 + a_1^2r^2)U^2 = 16r^4 \quad (11)$$

Frequency responses of the linear and nonlinear cases with no saturation are plotted in Figure 6 for $a_1=0.2$, and $a_2=0.04$. Deviation of the spring from a fixed value and its dependence on the generalized displacement coordinate, introduces new features such as jump phenomenon (Stoker 1955).

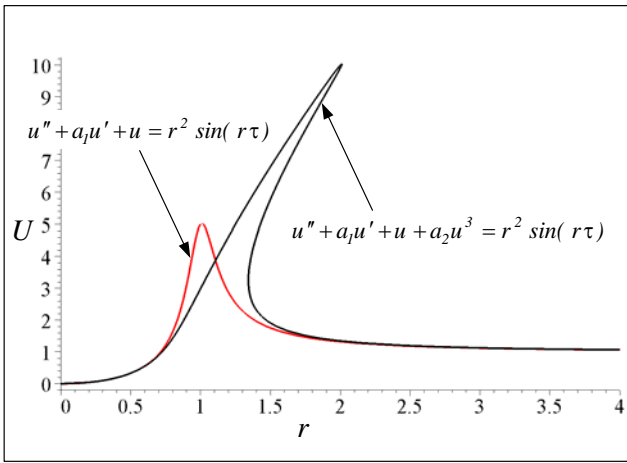


Figure 6: Frequency responses of the linear, and hardening spring for $a_1=0.2$, $a_2=0.04$.

2.2. Saturating Spring

The problem discussed in here is a base excited nonlinear vibration isolator with saturating spring with the following equation

$$u'' + a_1u' + u + a_2u^3 + a_3 \tanh(a_4u) = r^2 \sin(r\tau). \quad (12)$$

In order to investigate the frequency response of the system, we employ the averaging method. Then, we assume a solution in form of

$$u = U(\tau) \sin(\varphi(\tau)) \quad (13)$$

where

$$u' = U(\tau) r \cos(\varphi(\tau)) \quad (14)$$

$$\varphi(\tau) = r\tau + \psi(\tau). \quad (15)$$

Equations (13) and (14) imply

$$U' \sin \varphi + U \psi' \cos \varphi = 0 \quad (16)$$

and

$$u'' = rU' \cos \varphi - rU(r + \psi') \sin \varphi. \quad (17)$$

Substituting Equations (13), (14), and (17), into Equation (12) leads to

$$r(U' + a_1U) \cos \varphi + U(1 - r\psi') \sin \varphi + a_2U^3 \sin^3 \varphi + a_3f(u) = r^2 \sin(\varphi - \psi) \quad (18)$$

Solving Equations (16) and (18) for U' and ψ' , and simplifying, generate the following equations

$$rU' = (U(r^2 - 1) \sin \varphi + r^2 \sin(\varphi - \psi)) \cos \varphi \quad (19)$$

$$-(a_1Ur \cos \varphi + a_2U^3 \sin^3 \varphi + a_3f) \cos \varphi$$

$$rU\psi' = -(Ur^2 \sin \varphi - a_1Ur \cos \varphi - U - a_3f) \sin \varphi \quad (20)$$

$$-(r^2 \sin(\varphi - \psi) - a_2U^3 \sin^3 \varphi) \sin \varphi$$

The variables U' and ψ' are slowly varying with time, and we may assume that their average remain constant over a period of oscillation. Hence,

$$2\pi rU' = \int_0^{2\pi} [(U(r^2 - 1) \sin \varphi + r^2 \sin(\varphi - \psi)) \cos \varphi] d\varphi - \int_0^{2\pi} [(a_1Ur \cos \varphi + a_2U^3 \sin^3 \varphi + a_3f) \cos \varphi] d\varphi \quad (21)$$

$$= -\pi(a_1U + r \sin \psi) + \int_0^{2\pi} f(U \sin \varphi) \cos \varphi d\varphi$$

$$2\pi\psi'r = \int_0^{2\pi} [(U - Ur^2 \sin \varphi + a_1Ur \cos \varphi + a_3f) \sin \varphi] d\varphi + \int_0^{2\pi} [(-r^2 \sin(\varphi - \psi) + a_2U^3 \sin^3 \varphi) \sin \varphi] d\varphi \quad (22)$$

$$= \frac{\pi}{r} \left(\frac{3}{4}a_2U^3 + U(1 - r^2) - r^2 \cos \beta \right)$$

$$+ a_3 \int_0^{2\pi} f(U \sin \varphi) \sin \varphi d\varphi$$

where

$$f(U \sin \varphi) = \begin{cases} f_1(U \sin \varphi) & -\varphi_0 < \varphi < \varphi_0 \\ f_2(U \sin \varphi) & \varphi_0 < \varphi < \varphi_1 \\ a_3 & \varphi_1 < \varphi < \pi - \varphi_1 \\ f_2(U \sin \varphi) & \pi - \varphi_1 < \varphi < \pi - \varphi_0 \\ f_1(U \sin \varphi) & \pi - \varphi_0 < \varphi < \pi + \varphi_0 \\ f_3(U \sin \varphi) & \pi + \varphi_0 < \varphi < \pi + \varphi_1 \\ -a_3 & \pi + \varphi_1 < \varphi < 2\pi - \varphi_1 \\ f_3(U \sin \varphi) & 2\pi - \varphi_1 < \varphi < 2\pi - \varphi_0 \end{cases} \quad (23)$$

and

$$f_1(x) = a_4 x - \frac{1}{3} a_4^3 x^3 \quad (24)$$

$$f_2(x) = a_4^3 x^3 \frac{Z_1}{Z_2} + a_4^2 x^2 \frac{Z_3}{Z_4} + a_4 x \frac{Z_5}{Z_6} + a_4 \frac{Z_7}{Z_8} \quad (25)$$

$$f_3(x) = a_4^3 x^3 \frac{Z_1}{Z_2} + a_4^2 x^2 \frac{Z_9}{Z_4} + a_4 x \frac{Z_5}{Z_6} + a_4 \frac{Z_{10}}{Z_8} \quad (26)$$

Z_1 to Z_{10} can be found in Appendix. Also we define

$$\varphi_0 = \sin^{-1} \left(\frac{\delta_0}{U} \right), \quad \delta_0 = 0.6 \quad (27)$$

$$\varphi_1 = \sin^{-1} \left(\frac{\delta_1}{U} \right), \quad \delta_1 = 2.0. \quad (28)$$

At steady state conditions, the left hand side of Equations (21) and (22) should be considered zero. Evaluation of the integrals

$$\int_0^{2\pi} f(U \sin \varphi) \cos \varphi d\varphi, \int_0^{2\pi} f(U \sin \varphi) \sin \varphi d\varphi \quad (29)$$

on the right hand side of Equations (21) and (22) must be carried on in three steps.

Step 1. In the first step we assume $U \leq \delta_0$. Then, φ_0 and φ_1 do not exist, and the saturating spring will never pass the limits of applicability of the principal expanded function about zero. The integrals must be evaluated using $f = f_1$ for entire the cycle of integration. The solution in the first step is valid as long as $0 < U \leq \delta_0$.

Then the results of the averaging method would be

$$r \sin \psi = -a_1 U \quad (30)$$

$$r^2 \cos(\psi) = U \left(1 - r^2 + a_3 a_4 \right) + \frac{1}{4} U^3 \left(3a_2 - a_3 a_4^3 \right) \quad (31)$$

Hence, the frequency response, and phase angle of the motion are

$$Z_{11} r^4 + Z_{12} r^2 + Z_{13} = 0 \quad (32)$$

$$\tan(\psi) = \frac{-ra_1}{\left(1 - r^2 + a_3 a_4 \right) + \frac{1}{4} U^2 \left(3a_2 - a_3 a_4^3 \right)} \quad (33)$$

where Z_{11} , Z_{12} and Z_{13} can be found in Appendix.

Step 2. In the second step we assume $0 < U \leq \delta_1$. Then, no φ_1 exist, and the saturating spring will never saturate, but it goes beyond the validity of the principal expanded function about zero. So, the integrals must be evaluated using $f = f_1$, $f = f_2$ and $f = f_3$ in the cycle of integration. The solution in the second step is valid as long as $\delta_0 < U \leq \delta_1$. Hence, we have

$$r \sin \psi = -a_1 U \quad (34)$$

$$\pi r^2 \cos(\psi) = \pi(1-r^2)U + \frac{1}{Z_{15}}(Z_{16}U^3 + Z_{17}U^2 + Z_{18}U + Z_{19}) \quad (35)$$

which can be used to get the implicit equations for the amplitude a , and phase ψ , as functions of the excitation frequency r .

$$\left(\pi a_1 r Z_{15} U \right)^2 + \left[-Z_{16} U^3 - Z_{17} U^2 + \left(\pi Z_{15} (r^2 - 1) - Z_{18} \right) U - Z_{19} \right]^2 = 1 \quad (36)$$

$$\tan(\psi) = \frac{\pi a_1 r Z_{14} U}{-Z_{15} U^3 - Z_{16} U^2 + \left(\pi Z_{14} (r^2 - 1) - Z_{17} \right) U - Z_{18}} \quad (37)$$

Z_{14} to Z_{18} are indicated in the appendix. Equation (36) is the required frequency response function that can be utilized to attain the dimensionless amplitude U at frequency r , or vice versa.

Step 3. In the third step, we assume $\delta_j < U$. Then, both variables φ_0 and φ_1 must be considered, and the integrals must be evaluated using Equation (23). The solution in the third step is valid as long as $\delta_j < U$.

$$r \sin \psi = -a_1 U \quad (38)$$

$$\begin{aligned} \pi r^2 \cos(\psi) &= \pi(1-r^2)U + 4a_3 \cos(\varphi_1) \\ &+ \frac{1}{Z_{19}}(Z_{20}U^3 + Z_{21}U^2 + Z_{22}U + Z_{23}) \end{aligned} \quad (39)$$

Z_{19} to Z_{23} are defined in Appendix.

2.3. Piecewise Linear Saturating Spring

In order to evaluate the importance of having a smooth saturating function compared to a simple approximation, in this section we assume a piecewise linear model instead of hyperbolic tangent function. Frequency response analysis of smooth saturating model produces a set of complicated equations. Therefore, we must evaluate the trade off between working with simpler model and the accuracy.

Using piecewise linear approximation, the equation of motion would be

$$u'' + a_1 u' + u + a_2 u^3 + a_3 f(u) = r^2 \sin(r\tau). \quad (40)$$

where

$$f(u) = \begin{cases} 1 & u > \frac{1}{a_4} \\ a_4 u & |u| \leq \frac{1}{a_4} \\ -1 & u < -\frac{1}{a_4} \end{cases}. \quad (41)$$

Applying the averaging method will produce the following implicit equations for frequency response and phase of the system.

$$\begin{aligned} &16\pi^2 r^2 a_1^2 U^2 - 16\pi^2 r^4 \\ &+ \left(4a_3 a_4 (2\varphi_0 - \sin 2\varphi_0) + \pi(3a_2 U^2 - 4r^2 + 4)\right)^2 U^2 \\ &+ (+16a_3 \cos \varphi_0)^2 U^2 = 0 \end{aligned} \quad U > \frac{1}{a_4} \quad (42)$$

$$\begin{aligned} \tan(\psi) &= -4a_1 U r \pi / \left[3a_2 U^3 \pi + 16a_3 \cos \varphi_0 \right. \\ &\quad \left. - 4a_1 U (r^2 - 1) \pi - 8a_3 a_4 U (\cos \varphi_0 - \varphi_0) \right] \end{aligned} \quad (43)$$

$$\begin{aligned} &16r^2 a_1^2 U^2 - 16r^4 \\ &+ \left(4a_3 a_4 + 3a_2 U^2 - 4r^2 + 4\right)^2 U^2 = 0 \quad U \leq \frac{1}{a_4} \end{aligned} \quad (44)$$

$$\tan(\psi) = \frac{-4a_1 U r}{(-4U(r^2 - 1) + 3a_2 U^3 + 4a_3 a_4 U)} \quad (45)$$

where

$$\varphi_0 = \sin^{-1} \left(\frac{1}{a_4} \right). \quad (46)$$

3. RESULTS

Figure 7 depicts the frequency response of the system for different coefficient of the saturating term. The resonance frequency shifts to the higher frequencies by increasing the strength of the saturation. The peak of frequency response also increases by increasing the saturation strength. The effects of the variation of switching amplitude are illustrated in Figure 8.

Frequency response of the system employing continuous nonlinear saturating and piecewise linear saturating models are compared in Figure 9, for a set of parameters that produces an observable difference. It is seen that the frequency response of the system utilizing the piecewise linear saturating model detects the dynamic of the system and shows the same trend of the steady state.

Further analysis can be examined by comparing analytic equations derived in the previous section. Effect of varying a_3 and a_4 are illustrated in Figure 10 and 11 respectively.

A sample of the phase angle of the steady state response is depicted in Figure 12, using the piecewise linear model. Nonlinear behavior and jumping phenomenon can be seen clearly.

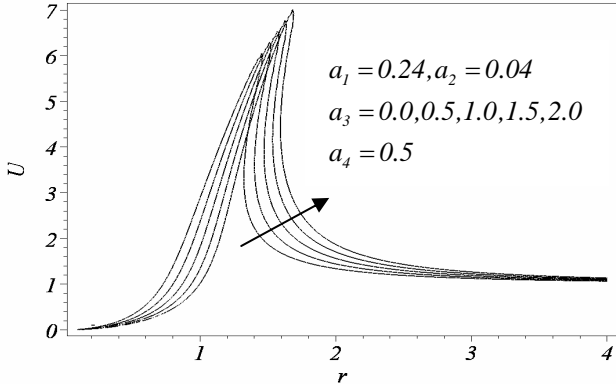


Figure 7: Effect of a_3 to relative displacement frequency response of the nonlinear saturating spring isolator.

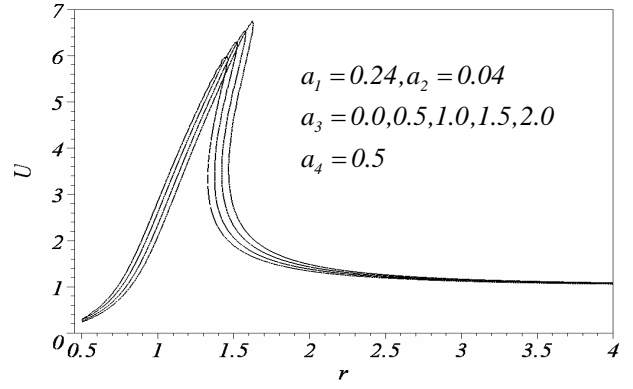


Figure 10: Effect of a_3 to relative displacement frequency response of the piecewise linear saturating spring isolator.

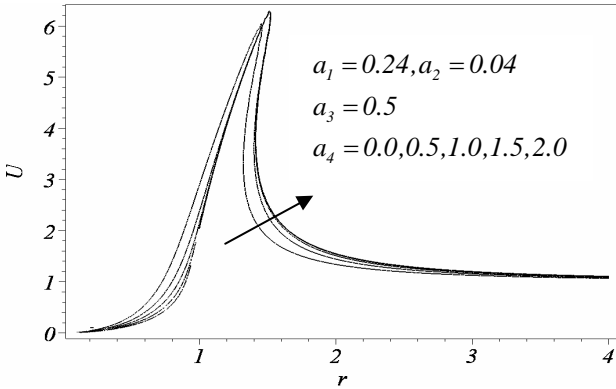


Figure 8: Effect of a_4 to relative displacement frequency response of the nonlinear saturating spring isolator.

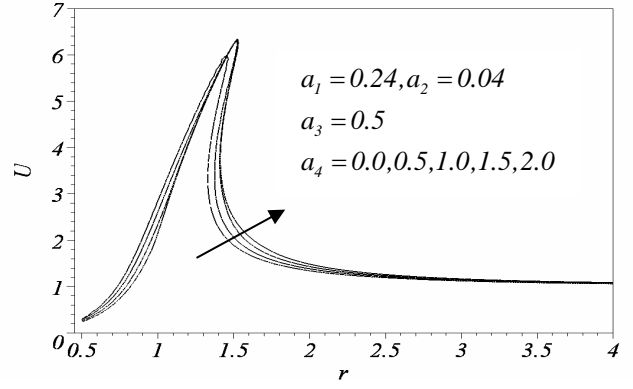


Figure 11: Effect of a_4 to relative displacement frequency response of the piecewise linear saturating spring isolator.

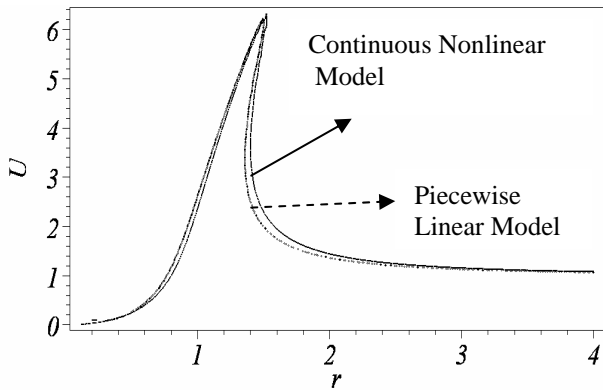


Figure 9: Comparison of relative displacement frequency response of piecewise linear and nonlinear saturating spring for $a_1=0.24$, $a_2=0.04$, $a_3=0.5$, $a_4=0.5$.

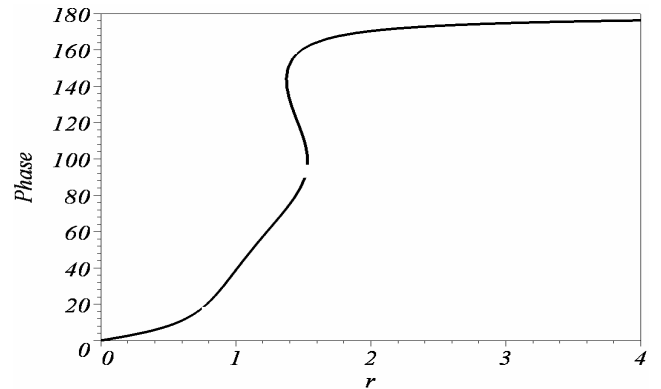


Figure 12: Phase of relative displacement frequency response of piecewise linear saturating spring for $a_1=0.2$, $a_2=0.04$, $a_3=0.5$, $a_4=0.5$.

CONCLUSION

A nonlinear suspension system has been studied, including a cubic restoring force element, a linear viscous damper, and a saturating restoring stiffness. Applying the averaging perturbation method, analytic equation has been derived to describe the steady state behavior of the system in various condition of the response. A simple parametric study verified the applicability of the analytic results.

The analysis has been done for a continuous (modeled by five nonlinear polynomial functions) and a piecewise linear model. Applying the averaging method to the continuous saturating function needed a careful analysis in every different step. The derived equations are cumbersome, long, complicated, and hard to work with. The analytic equation for describing the steady state behavior of the system has also been derived using a simpler model of piecewise linear saturating stiffness. The investigation has shown that the piecewise linear model generates much simpler analytic results, with reasonably close results. Therefore, the corresponding equations may be utilized for further investigation on saturating stiffness.

REFERENCES

- Chabota, M. D., and Moreland, J., (2003) "Micrometer-scale magnetometry of thin Ni80Fe20 films using ultrasensitive microcantilevers", *Journal of Applied Physics*, **93**(10), 7897-9.
- Den Hartog J. P., and Mikina S. J., (1932), "Forced Vibrations with Nonlinear Spring Constraints," *Trans. ASME, Applied Mechanics*, **54-APM-15**, pp. 157.
- Fleishman B. A., (1965), "Forced Oscillations and Convex Superposition in Piecewise Linear Systems," *SIAM Review*, **7**(2), 205-222.
- Jolly, M. R., Carlson, J. D., and Munoz, B. C., 1996, "A Model of the Behavior of Magnetorhological Materials," *Journal of Smart Mater. Struct.*, No. 5, 607-614.
- Maezawa S., (1961), "A Perfect Fourier Series Solution for the Steady Forced Vibration of a Piecewise Linear System," *Proc. Int. Symp. On Nonlinear Oscillations*, Kiev, vol. I, 327-341.
- Nayfeh, A. H., Mook, D. T., (1979), "Nonlinear oscillations", *John Wiley & Sons*.

Schmidt, G., & Tondle, A., (1986), "Non-linear vibrations", *Akademie, Berlin*.

Stoker, J.J., (1955), "Nonlinear Vibrations in Mechanical and electrical systems", *John Wiley & Sons*.

Tai, C., Stubbs, A., and Tsao, T.C., (2001), "Modeling and Controller Design of an Electromagnetic Engine Valve", *Proceedings of American Control Conference*, 2890-2895.

True, H., and Asmund, R., (2002), "The dynamics of a railway freight wagon wheelset with dry friction damping", *Vehicle System Dynamics*, **38**,149-163.

Walsh, P. L., and Lamancusa, J. S., (1992), "Variable stiffness vibration absorber for minimization of transient vibrations", *Journal of Sound and Vibration*, **158**(2), 195-211.

APPENDIX

$$Z_1 = -0.03a_3^4 a_4^4 + 1.76 a_3^3 a_4^3 - 20.01a_3^2 a_4^2 + 25 a_3 a_4 + 106.97$$

$$Z_2 = 0.1a_3^4 a_4^4 - 5.29a_3^3 a_4^3 + 105.07 a_3^2 a_4^2 - 926.96 a_3 a_4 + 3066.67$$

$$Z_3 = -11.0a_3^5 a_4^5 - 6.0a_3^3 a_4^3 + 85.19a_3^2 a_4^2 - 1004.0$$

$$Z_4 = 0.1a_3^4 a_4^4 - 5.29a_3^3 a_4^3 + 105.07 a_3^2 a_4^2 - 926.96 a_3 a_4 + 3066.67$$

$$Z_5 = 0.70a_3^4 a_4^4 - 5.29a_3^3 a_4^3 - 30.43a_3^2 a_4^2 - 525.35 a_3 a_4 + 3066.67$$

$$Z_6 = 0.1a_3^4 a_4^4 - 5.29a_3^3 a_4^3 + 105.07 a_3^2 a_4^2 - 926.96 a_3 a_4 + 3066.67$$

$$Z_7 = -1.13a_3^3 a_4^3 + 18.06 a_3^2 a_4^2 - 40.16 a_3 a_4$$

$$Z_8 = 0.1a_3^4 a_4^4 - 5.29a_3^3 a_4^3 + 105.07 a_3^2 a_4^2 - 926.96 a_3 a_4 + 3066.67$$

$$Z_9 = -6.0a_3^3 a_4^3 + 85.19a_3^2 a_4^2 - 1004.0$$

$$Z_{10} = -1.13a_3^3 a_4^3 + 18.06 a_3^2 a_4^2 - 40.16 a_3 a_4$$

$$Z_{11} = U^2 - 1$$

$$Z_{12} = \frac{1}{2}(a_3 a_4 - 3a_2)U^4 + (a_1^2 - 2a_3 a_4 - 2)U^2$$

$$Z_{13} = \frac{1}{16}(a_3 a_4^3 - 3a_2)^2 U^6 + \frac{1}{2}((a_3 - 1)a_3 a_4^4 + 3a_2 a_3 (a_4 + 1))U^4 + (1 + a_3 a_4)^2 U^2$$

$$Z_{14} = 0.125 a_3^4 a_4^4 - 6.616 a_3^3 a_4^3 + 131.339 a_3^2 a_4^2 - 1158.699 a_3 a_4 + 3833.342$$

$$Z_{15} = \frac{3}{4} a_2 \pi + \frac{1}{2} a_3 a_4^3 \Phi_0 - \frac{1}{4} a_3 a_4^3 \sin(2\Phi_0) + \frac{1}{6} a_3 a_4^3 \sin^2(\Phi_0) \sin(2\Phi_0) + \frac{1}{6} a_3 a_4 \left([1890.254 a_4^2 + 441.786 a_3 a_4^3 - 353.639 a_3^2 a_4^4 + 31.180 a_3^3 a_4^5 - 0.589 a_3^4 a_4^6 + 18.761 a_4^4 a_3^2] \sin(\Phi_0) + [-1203.373 a_4^2 - 281.250 a_3 a_4^3 + 225.134 a_3^2 a_4^4 - 19.849 a_3^3 a_4^5 + 0.375 a_3^4 a_4^6] \Phi_0 + [802.248 a_4^2 + 187.50 a_3 a_4^3 - 150.089 a_3^2 a_4^4 + 13.233 a_3^3 a_4^5 - 0.250 a_3^4 a_4^6] \sin(2\Phi_0) + [-100.281 a_4^2 - 23.437 a_3 a_4^3 - 1.654 a_3^3 a_4^5 + 0.031 a_3^4 a_4^6] \sin(4\Phi_0) \right)$$

$$Z_{16} = \frac{1}{6} a_3 a_4 \left([-22590.099 a_4 + 1916.908 a_3^2 a_4^3 - 135.107 a_3^3 a_4^4] \cos(\Phi_0) + [2510.011 a_4 - 212.989 a_3^2 a_4^3 + 15.011 a_3^3 a_4^4] \cos(3\Phi_0) \right)$$

$$Z_{17} = \frac{1}{6} a_3 a_4 (72256.810 - 12378.448 a_3 a_4 - 717.023 a_3^2 a_4^2 - 124.720 a_3^3 a_4^3 + 16.504 a_3^4 a_4^4 + [-46000.114 + 7880.365 a_3 a_4 + 456.471 a_3^2 a_4^2 + 79.399 a_3^3 a_4^3 - 10.507 a_3^4 a_4^4] \Phi_0 + [23000.057 - 3940.182 a_3 a_4 - 228.235 a_3^2 a_4^2 - 39.699 a_3^3 a_4^3 + 5.253 a_3^4 a_4^4] \sin(2\Phi_0))$$

$$Z_{18} = \frac{1}{6} a_3^2 a_4^2 [-34.078 a_3^3 a_4^2 + 542.011 a_3^2 a_4 - 1204.805 a_3] \cos(\Phi_0)$$

$$Z_{19} = 0.125 a_3^4 a_4^4 - 6.6164 a_3^3 a_4^3 + 131.339 a_3^2 a_4^2 - 1158.699 a_3 a_4 + 3833.342$$

$$Z_{20} = \frac{3}{4} a_2 \pi - \frac{1}{3} a_4^2 \sin^2(\Phi_0) \sin(2\Phi_0) - \frac{1}{3} a_3 a_4 \left([603.186 a_4^2 + 140.625 a_3 a_4^3 - 112.567 a_3^2 a_4^4 + 9.924 a_4^5 a_3^3 a_4^5 - 0.187 a_3^4 a_4^6] \Phi_0 + [-601.686 a_4^2 - 140.625 a_3 a_4^3 + 112.567 a_3^2 a_4^4 - 9.924 a_3^3 a_4^5 + 0.1875 a_3^4 a_4^6] \Phi_1 + [-401.290 a_4^2 - 93.750 a_3^1 a_4^3 + 75.044 a_3^2 a_4^4 - 6.616 a_3^3 a_4^5 + 0.125 a_3^4 a_4^6] \sin(2\Phi_0) + [401.124 a_4^2 + 93.750 a_3^1 a_4^3 - 75.044 a_3^2 a_4^4 + 6.616 a_3^3 a_4^5 - 0.125 a_3^4 a_4^6] \sin(2\Phi_1) + [50.140 a_4^2 + 11.718 a_3^1 a_4^3 - 9.380 a_3^2 a_4^4 - 0.827 a_3^3 a_4^5 - 0.015 a_3^4 a_4^6] \sin(4\Phi_0) + [-50.140 a_4^2 - 11.718 a_3^1 a_4^3 + 9.380 a_3^2 a_4^4 - 0.827 a_3^3 a_4^5 + 0.015 a_3^4 a_4^6] \sin(4\Phi_1) \right)$$

$$\begin{aligned}
Z_{21} = & -\frac{1}{3}a_3a_4 \left(\left[11295.049a_4 - 958.454a_3^2a_4^3 \right. \right. \\
& + 67.553a_3^3a_4^4 \left. \left. \right] \cos(\varphi_0) + \left[-11295.049a_4 \right. \right. \\
& + 958.4543a_3^2a_4^3 - 67.553a_3^3a_4^4 \left. \left. \right] \cos(\varphi_1) \right. \\
& + \left[-1255.005a_4 + 106.494a_3^2a_4^3 - 7.505a_3^3a_4^4 \right] \cos(3\varphi_0) \\
& \left. + \left[1255.005a_4 - 106.494a_3^2a_4^3 + 7.505a_3^3a_4^4 \right] \cos(3\varphi_1) \right)
\end{aligned}$$

$$\begin{aligned}
Z_{22} = & -\frac{1}{3}a_3a_4 \left(\left[602.402a_3^2a_4^2 - 271.005a_3^3a_4^2 \right. \right. \\
& + 17.039a_3^4a_4^3 \left. \left. \right] \cos(\varphi_0) + \left[-17.039a_3^4a_4^3 \right. \right. \\
& - 602.402a_3^2a_4^2 + 271.005a_3^3a_4^2 \left. \left. \right] \cos(\varphi_1) \right)
\end{aligned}$$

$$\begin{aligned}
Z_{23} = & -\frac{1}{3}a_3a_4 \left(\left[2298.057 - 3940.182a_3a_4 \right. \right. \\
& - 228.235a_3^2a_4^2 - 39.699a_3^3a_4^3 + 5.253a_3^4a_4^4 \left. \left. \right] \varphi_0 \right. \\
& + \left[-23000.057 + 3940.182a_3a_4 + 228.235a_3^2a_4^2 \right. \\
& + 39.699a_3^3a_4^3 - 5.253a_3^4a_4^4 \left. \left. \right] \varphi_1 + \left[-11498.028 \right. \right. \\
& + 1970.091a_3a_4 + 114.117a_3^2a_4^2 + 19.849a_3^3a_4^3 \\
& - 2.626a_3^4a_4^4 \left. \left. \right] \sin(2\varphi_0) + \left[11500.028 - 1970.091a_3a_4 \right. \right. \\
& - 114.117a_3^2a_4^2 - 19.849a_3^3a_4^3 + 2.626a_3^4a_4^4 \left. \left. \right] \sin(2\varphi_1) \right)
\end{aligned}$$